PHYSICAL REVIEW B, VOLUME 63, 060503(R)

Quasi-two-dimensional Fermi surfaces of the heavy fermion superconductor $CeIrIn_5$

Yoshinori Haga,[1] Yoshihiko Inada,[2] Hisatomo Harima,[3] Kenichi Oikawa,[4] Masao Murakawa,[2] Hirokazu Nakawaki,[2] Yoshihumi Tokiwa,[1,2] Dai Aoki,[2] Hiroaki Shishido,[2] Shuugo Ikeda,[2] Narumi Watanabe,[2] and Yoshichika Onuki[1,2]

[1]*Advanced Science Research Center, Japan Atomic Energy Research Institute, Tokai, Ibaraki 319-1195, Japan*

[2]*Graduate School of Science, Osaka University, Toyonaka, Osaka 560-0043, Japan*

[3]*The Institute of Scientific and Industrial Research, Osaka University, Ibaraki 567-0047, Japan*

[4]*National Institute of Materials and Chemical Research, Tsukuba 305-8565, Japan*

(Received 9 November 2000; published 17 January 2001)

We observed the de Haas–van Alphen oscillation in the heavy fermion compound $CeIrIn_5$. The topology of the Fermi surface is found to be nearly cylindrical, reflecting the unique tetragonal structure. Observed branches are well explained by the $4f$-itinerant band model. The cyclotron masses of $20-30m_0$ are one order larger than the corresponding band masses.

DOI: 10.1103/PhysRevB.63.060503 PACS number(s): 74.70.Tx, 71.18.+y, 71.27.+a

The de Haas–van Alphen (dHvA) effect is a powerful method of determining the topology of the Fermi surface, the cyclotron effective mass m_c^*, and the scattering lifetime τ in metals. This phenomenon was studied in the strongly correlated electron systems of the rare-earth and uranium compounds, or so-called heavy fermion compounds.[1] In fact, the heavy mass of about $100m_0$ (m_0: the rest mass of an electron) was detected by the dHvA effect in $CeRu_2Si_2$ (Ref. 2) and UPt_3.[3,4]

In cerium compounds, both the Ruderman-Kittel-Kasuya-Yosida (RKKY) interaction and the Kondo effect compete with each other. The RKKY interaction induces the long-range magnetic order, while the magnetic moment of a $4f$ electron is compensated by the conduction electron spin polarization via the Kondo effect. When the Kondo effect overcomes the RKKY interaction at low temperatures, the heavy fermion state is formed, e.g., as in $CeRu_2Si_2$ indicating no long-range magnetic order. Most of the cerium compounds, however, exhibit the magnetic order. Interesting is a pressure effect on a Néel temperature T_N in antiferromagnetic cerium compounds such as $CeIn_3$ or $CePd_2Si_2$.[5] When pressure p is applied to these cerium compounds, T_N shifts to lower temperatures, and the magnetic quantum critical point, corresponding to the extrapolation $T_N \to 0$, is reached at $p=p_c$. Superconductivity appears around p_c. Correspondingly, the heavy fermion state is formed around p_c.

Recently it was reported that $CeRhIn_5$ is a pressure-induced superconductor.[6] $CeRhIn_5$ is an antiferromagnet with $T_N=3.8$ K at ambient pressure. Superconductivity was observed at $p>16$ kbar, although the decay of the magnetic order is not simple.

A similar compound $CeIrIn_5$ is also a heavy fermion superconductor with a transition temperature $T_c=0.4$ K at ambient pressure and a large electronic specific heat coefficient $\gamma=750\,\mathrm{mJ/K^2\cdot mol}$.[7] This is the second case among the heavy fermion cerium compounds, where superconductivity was found at ambient pressure only in $CeCu_2Si_2$ with $\gamma=1000\,\mathrm{mJ/K^2\cdot mol}$.[8] Both $CeRhIn_5$ and $CeIrIn_5$ have the $HoCoGa_5$-type tetragonal crystal structure ($P4/mmm$ $\#123\,D_{4h}^1$) with alternating layers of $CeIn_3$ and $Rh(Ir)In_2$ stacked sequentially along the [001] direction (c axis), as shown in Fig. 1.

$CeIrIn_5$ in the normal state is the heavy fermion compound, similar to $CeRu_2Si_2$. The large γ value corresponds to the large effective mass. Moreover, the Brillouin zone becomes flat along the [001] direction, reflecting a large lattice constant c. These characteristic features might bring about the peculiar Fermi surface properties in $CeIrIn_5$, namely a two-dimensional character. We have thus done the dHvA experiment. The experimental result is compared to the result of the full potential linear augmented plane wave (FLAPW) band calculations.

Single crystals of $CeIrIn_5$ were grown by the so-called

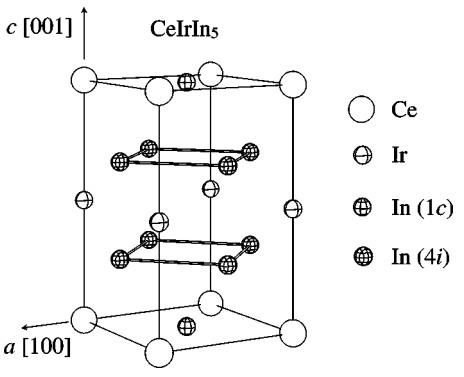

FIG. 1. Crystal structure in $CeIrIn_5$.

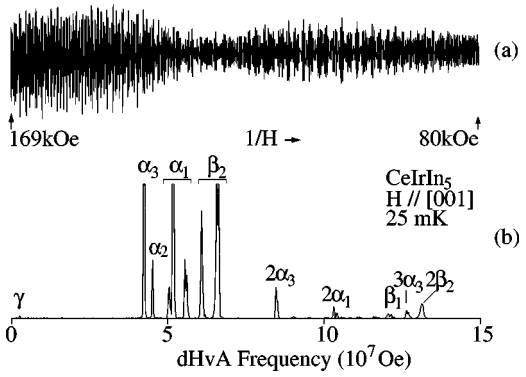

FIG. 2. (a) Typical dHvA oscillation for the field along [001] and (b) the corresponding FFT spectrum in $CeIrIn_5$.

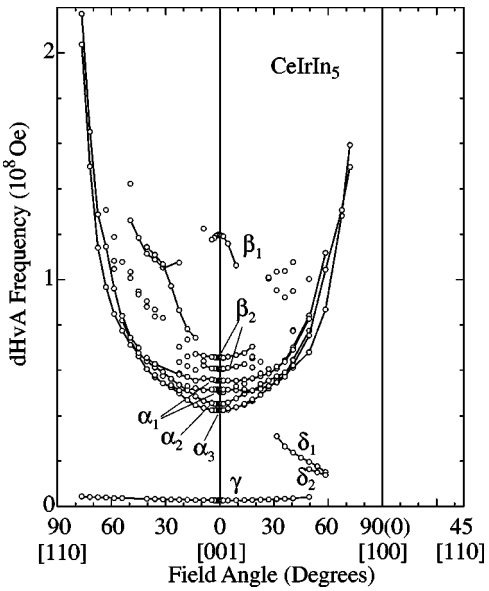

FIG. 3. Angular dependence of the dHvA frequency in $CeIrIn_5$.

self-flux method as described in Ref. 6. The x-ray powder diffraction measurement was carried out at room temperature using the Cu-Kα radiation monochromatized with a curved graphite. Diffraction intensities were well explained by the $HoCoGa_5$-type structure mentioned above. Lattice parameters, obtained from the Rietveld refinement, were $a = 4.6662$ Å and $c = 7.5168$ Å. Fractional coordinates of indium at the $4i$ site were determined as (0,0.5,0.3053). These lattice parameters are compared to $a = 4.652$ Å and $c = 7.542$ Å in $CeRhIn_5$, suggesting that $CeIrIn_5$ corresponds to the pressure-induced $CeRhIn_5$.

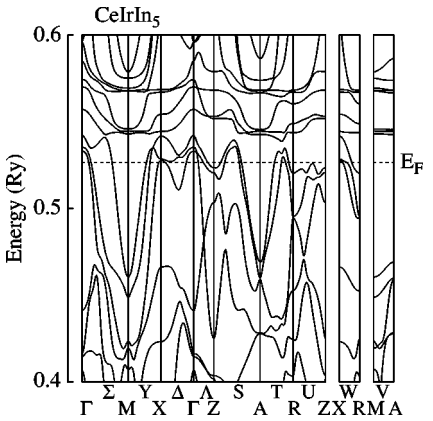

FIG. 4. Energy band structure in $CeIrIn_5$.

The temperature dependence of the electrical resistivity ρ is typical for a heavy fermion system and resembles that observed for $CeRu_2Si_2$. There is also found a large anisotropy in the resistivity. A value of $\rho_{[001]}/\rho_{[100]}$ at room temperature is about 3.5, and increases slightly to 4.5 at 4.2 K. This anisotropy is closely related to the quasi-two-dimensional Fermi surface, mentioned later. The electrical resistivity drops at about 1 K and becomes zero at lower temperatures, indicating superconductivity. The resistivities at 1.5 K and room temperature are 5.2 and 89 $\mu\Omega$ cm, respectively, in the current along [100].

Next we measured the dHvA oscillation using a so-called 2ω detection of the field modulation method.[1] Figure 2 shows the typical dHvA oscillation for the field along [001] at 25 mK and the corresponding fast Fourier transformation (FFT) spectrum. There are detected eight dHvA branches

TABLE I. de Haas–van Alphen frequency F, the cyclotron effective mass m_c^*, the Dingle temperature T_D and the mean-free path l in $CeIrIn_5$.

	Experimental				Theoretical		
$H\|\|[001]$	$F(\times 10^7$ Oe)	$m_c^*(m_0)$	T_D (K)	l (Å)		$F(\times 10^7$ Oe)	$m_b(m_0)$
					a (band 15)	15.2	4.89
					c (band 14)	12.8	3.95
β_1	12.0	32			β_1(band 14)	12.4	3.32
β_2	6.59	21	0.29	1050	β_2(band 14)	6.18	1.33
	6.11	30				6.18	1.37
						6.16	1.27
α_1	5.56	25			α_1(band 15)	5.00	1.89
	5.15	17					
	5.07	23					
α_2	4.53	29			α_2(band 15)	4.03	1.15
α_3	4.24	10			α_3(band 15)	3.65	1.37
					d (band 14)	1.00	1.68
					g (band 13)	0.70	0.64
γ	0.27	6.3	0.35	580			
					h (band 13)	0.14	1.04
$H\|\|49.5°$ from [001] to [100]							
δ_1	1.96	45	0.02	4500	(band 14)	2.29	2.17
δ_2	1.63	35	0.08	1100	(band 14)	2.08	3.14

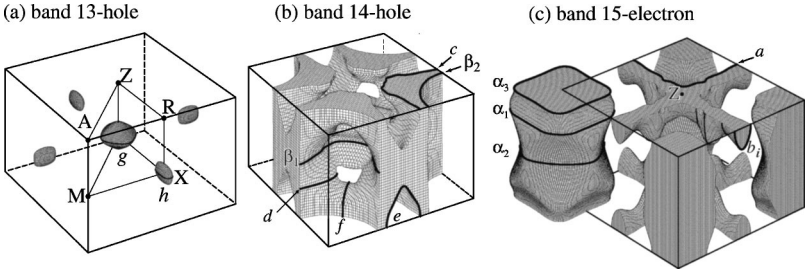

FIG. 5. Fermi surfaces of $CeIrIn_5$.

named α_i, β_i, and γ as well as their higher harmonics. When the field is tilted from [001] to [100] and [110], dHvA frequencies of branches α_i ($i=1$, 2, and 3) roughly follow a $1/\cos\theta$ dependence, where the dHvA frequency F ($=\hbar S_F/2\pi e$) is proportional to the extremal (maximum or minimum) cross-sectional area S_F of the Fermi surface. This angular dependence indicates the existence of a cylindrical Fermi surface. The other branches are observed mainly in a region around [001]. The angular dependence of these branches is shown in Fig. 3. We note that the dHvA signal due to an In flux was not observed.

The cyclotron mass m_c^* was determined from the temperature dependence of the dHvA amplitude. It is in the range from 6.3 to $45\,m_0$. A large cyclotron mass is surely observed in $CeIrIn_5$. The Dingle temperature T_D $[=(\hbar/2\pi k_B)\tau^{-1}]$, where τ is the scattering lifetime, was also determined from the field dependence of the dHvA amplitude. It is in the range from 0.017 to 0.35 K. We can thus estimate the mean free path l by using the following formulas: $S_F=\pi k_F^2$, $\hbar k_F=m_c^* v_F$, and $l=v_F\tau$, where the wave number k_F is half of the caliper dimension of a simple circular area S_F and v_F is Fermi velocity. The mean-free path l is in the range from 580 to 4500 Å, indicating high quality of the sample. These values are summarized in Table I.

We calculated the energy band structure of $CeIrIn_5$ in the scheme of the FLAPW method within the local-density approximation. The $4f$ electrons in $CeIrIn_5$ are assumed to be itinerant. The $5s^25p^6$ electrons for Ce, $5p^6$ for Ir and $4d^{10}$ for In are treated as semicore electrons and the other deeper electrons are calculated in the Muffin Tin spheres as core electrons in each iterative process. The linear augmented plane wave (LAPW) basis functions are truncated at $|\mathbf{k}+\mathbf{G}_i|\leqslant 4.85(2\pi/a)$, where $\mathbf{G}_i$ is the reciprocal lattice vector and a is the lattice constant, corresponding to 771 LAPW's at the Γ points. We used 112 and 637 sampling k points in the irreducible 1/16th Brillouin zone for potential convergence and a final band structure, respectively. Figure 4 shows the energy band structure along the symmetry axes. The $5d$ electrons of Ir hybridize with the $5p$ electrons of In $(4i)$, forming bonding and antibonding bands, which results in a small density of states around the Fermi energy E_F. This means that there are scarcely conduction electrons in the Ir layers. This is reflected in the band structure with no dispersion along *AM*, indicating the existence of a quasi-two-dimensional Fermi surface. The Fermi surfaces are thus produced by the $5d$ and $4f$ electrons of Ce and $5p$ electrons of In ($4i$ site). The contribution of $4f$ component to the density of states is about 60% at E_F.

The calculated Fermi surfaces are shown in Fig. 5. The band 13-hole Fermi surface consists of an ellipsoidal Fermi surface centered at the X points and a flat ''cushion''-like Fermi surface centered at the Γ point. The band 14-hole Fermi surface is, however, not a closed Fermi surface, elongated along [001]. The band 15-Fermi surface is a compensated electron Fermi surface, consisting of a cylindrical one and a networklike lattice. $CeIrIn_5$ is thus a compensated metal with equal numbers of electron and hole carriers.

Figure 6 shows the angular dependence of the theoretical dHvA frequency. The origin of the dHvA branches in Fig. 6 is explained on the basis of the $4f$-itinerant band model. Branches α_i are due to extremal orbits of the cylindrical band 15-electron Fermi surface. Five branches are observed experimentally, although theoretically the number of branches α_i is three, as shown in Fig. 5(c). The cyclotron masses are about $20\,m_0$, which are one order larger than the band masses. We note that orbits named a and b_i in the ''lattice''-Fermi surface in Fig. 5(c) are not observed experimentally. Branches β_i are due to inner orbits of the band 14-hole Fermi surface in Fig. 5(b), although an outer orbit named c is not observed. This might be ascribed to the damping of the dHvA amplitude due to the curvature factor of the Fermi surface and/or a large cyclotron mass of $50-100m_0$, expected from the γ value. The cyclotron masses of branches β_i in Table I are also one order larger than the corresponding band masses. Here we note that two branches β_2 are observed, whereas theoretically three ex-

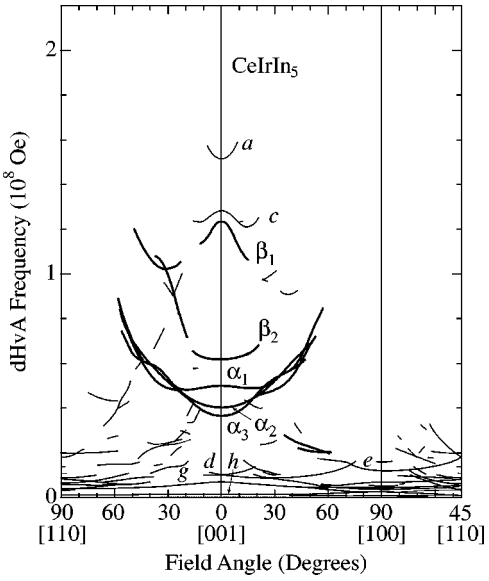

FIG. 6. Angular dependence of the theoretical dHvA frequency in $CeIrIn_5$.

tremal orbits are almost degenerated. Anyway, splitting of branches α_i and β_i, which is reflected as the beats in the dHvA oscillation, is mainly due to the corrugated Fermi surfaces.

The origin of branch γ with $m_c^* = 6.3m_0$ is not clear. It might be ascribed to the closed Fermi surfaces named *g* or *h* in Fig. 5(a). Orbits named b_i, *e*, and *f* with low dHvA frequencies were not observed. This is mainly due to the present field modulation method.

The theoretical γ value is $\gamma_b = 28.2\,\mathrm{mJ/K^2 \cdot mol}$. The experimental γ value 750 $\mathrm{mJ/K^2 \cdot mol}$ is 25 times larger than the γ_b value, which is approximately consistent with the relation between the cyclotron mass and the band mass. Moreover, the cyclotron mass is found to be slightly field-dependent: $24m_0$ in 90–117 kOe and $20m_0$ in 117–169 kOe for branch β_2 ($F = 6.59 \times 10^7$ Oe). Here, the masses in Table I were mainly determined in the field range from 90 to 169 kOe.

The topology of the Fermi surface with a quasi-two-dimensional character is thus well explained by the $4f$-itinerant band model. The conduction electrons with large masses condense into the superconducting state. The upper critical field H_{c2} for superconductivity was reported to be anisotropic,[7] which is mainly due to the anisotropic Fermi surface. Namely, the so-called effective mass model based on the anisotropic mass is applicable to explain the angular dependence of H_{c2}.

This work was financially supported by COE Research (10CE2004) of the Ministry of Education, Science, Sports and Culture, Japan.

[1] Y. Ōnuki and A. Hasegawa, *Handbook on the Physics and Chemistry of Rare Earths*, edited by K. A. Gschneidner, Jr. and L. Eyring (Elsevier, Amsterdam, 1995), Vol. 20, p. 1.

[2] H. Aoki, S. Uji, A. K. Albessard, and Y. Onuki, Phys. Rev. Lett. **71**, 2110 (1993).

[3] S. R. Julian, P. A. A. Teunissen, and S. A. J. Wiegers, Phys. Rev. B **46**, 9821 (1992).

[4] N. Kimura, T. Tani, H. Aoki, T. Komatsubara, S. Uji, D. Aoki, Y. Inada, Y. Onuki, Y. Haga, E. Yamamoto, and H. Harima, Physica B **281&282**, 710 (2000).

[5] N. D. Mathur, F. M. Grosche, S. R. Julian, I. R. Walker, D. M. Freye, R. K. W. Haselwimmer, and G. G. Lonzarich, Nature (London) **394**, 39 (1998).

[6] H. Hegger, C. Petrovic, E. G. Moshopoulou, M. F. Hundley, J. L. Sarrao, Z. Fisk, and J. D. Thompson, Phys. Rev. Lett. **84**, 4986 (2000).

[7] J. L. Sarrao and R. Movshovich, in Proceedings of the American Physical Society, March, 2000 (AIP, Melville, NY, in press).

[8] F. Steglich, J. Aarts, C. D. Bredl, W. Lieke, D. Meschede, W. Franz, and H. Schäfer, Phys. Rev. Lett. **43**, 1892 (1979).